PHYSICAL REVIEW B VOLUME 15, NUMBER 2 15 JANUARY 1977

Theory of bound states induced by disorder and isoelectronic potentials: Ga(As,P):N

George G. Kleiman
Instituto de Fisica, Universidad Nacional Autonoma de Mexico, Mexico 20, D.F., Mexico and Instituto de Física, Universidade Estadual de Campinas, Campinas, São Paulo, Brazil*
(Received 24 May 1976)

A theory is presented in which bound states arising from a combination of long-range and short-range isoelectronic potentials are shown to account for recent experimental data in Ga(As,P):N. These results alter our physical picture in this system. Numerical calculations agree with experiment. They indicate that the long-range potential may correspond to a deformation potential which arises from a uniform, slowly varying dilation of the lattice constant in the region of the nitrogen atom. Analysis of experimental data suggests an expansion of 0.9% of the lattice constant.

I. INTRODUCTION

Motivated by practical considerations, a great deal of research has concentrated upon the fundamental luminescent properties of III–V mixed-crystal alloys containing nitrogen, an isoelectronic impurity. The system Ga(As, P):N (of which GaP is a component) has received most of this attention[1,2] because of the high quality of vapor-phase epitaxial crystals and the ease with which p-n junctions are fabricated.[1] From these studies, a picture of the properties of nitrogen in this system has emerged. The earliest experimental work,[2] in GaP, has shown that, because of its strong luminescent character in that indirect material, nitrogen is best described by a short-range electronic potential, with resulting delocalization in $\vec{k}$ space of the wave function. This has led to the conclusion[3] that the one-band one-site Koster-Slater approximation predicts (at least qualitatively) the features of the nitrogen state in GaP, which serves to justify its almost universal use in theoretical treatments.[3-9] Furthermore, experimental studies[2,10] in GaP containing a high nitrogen concentration (N) indicate that sharp structure arising from N-N pairs appears and the shape of the total photoluminescence spectrum manifests a marked dependence upon N. Extensions of these studies[1] into Ga(As, P) indicate[11,12] that N-dependent structure persists for $0.9 \lesssim x \lesssim 1$ (i.e., x is the mole fraction of P and $x = 1$ corresponds to GaP).

When, however, $x \lesssim 0.9$, the sharp N-N structure is replaced by a single broad peak which has been considered,[1,11,12] until recently, to be the envelope of the N-N pair structure broadened by disorder effects in the mixed crystal. Besides the broad N-N peak, there persists a line corresponding to that arising from single nitrogen atoms and which has been labeled the "A line."[1] Studies at still lower[4,11-14] x (i.e., near the direct-indirect crossover at $x = x_c$) indicate effects which have been interpreted within the Koster-Slater approximation.[15] The first of these is that of band-structure enhancement[2] (BSE), which predicts that the strong $\vec{k} = 0$ component of the short-range nitrogen state increases tremendously as the energy of the state approaches that of the $\vec{k} = 0$ band minimum (i.e., E_Γ). Another effect is that the state becomes resonant[4,5,13] for $x < x_c$.

The results of recent experiments,[16-18] however, suggest that much of the picture for $x < 0.9$ is incorrect. Systematic studies[16] indicate that the shape of the spectrum in this region is *not* a function of N, so that N-N contributions are unlikely. The measurements[16] imply that what had been identified as a broad N-N peak is, in fact, a strong phonon sideband of the single nitrogen state. Moreover, experiments[17,18] in the range $0.35 \lesssim x \lesssim 0.55$ display another peak, higher in energy than that arising from the single nitrogen. Pressure measurements[18] show that this state follows the Γ (direct) minimum for $x \lesssim 0.45$ and the X (indirect) minimum for $0.45 \lesssim x \lesssim 0.55$. Although these results, which alter our physical picture drastically, must be examined systematically, we accept them and present an explanation here. A brief version of some of these results has been published.[19]

In the theory presented here,[19] we show that these phenomena can be understood if there is a long-range, slowly varying potential (V_l) as well as the usual short-range potential (V_s), associated with the nitrogen atom. The only property we require of this potential is that it be strong enough (when $V_s = 0$) to produce bound states associated with both the X and Γ minima (in this work, we make the conventional[1] assumption that only the Γ and X minima are important). The energies of these states, denoted by N_X (energy W_{N_X}) and N_Γ (energy W_{N_Γ}), respectively, and the short range state, denoted by N (energy W_N), which appears when $V_l = 0$, are illustrated schematically as a function of x in Fig. 1(a). When these potentials are combined, the resulting energies are illustrated schematically in Fig. 1(b). Near the point where $W_N \simeq W_{N_\Gamma}$ the states

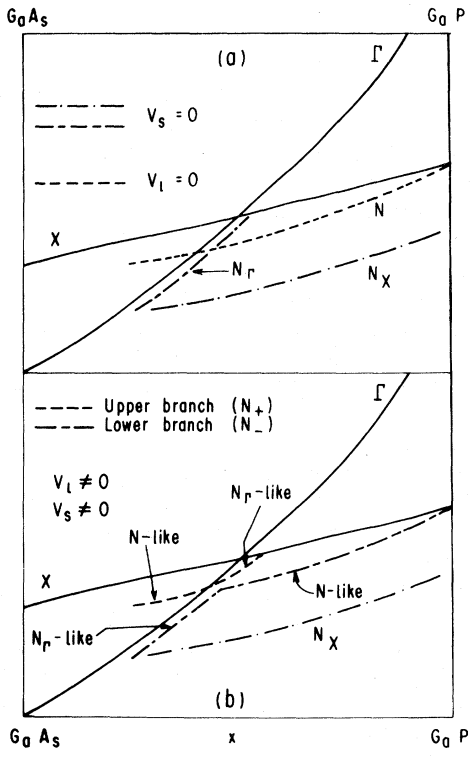

FIG. 1. (a) Schematic illustration of composition dependence of the energies of bound states associated with the $\Gamma(N_\Gamma)$ and $X(N_X)$ conduction-band minima which are produced by the long-range potential (V_l) in the absence of the short-range, isoelectronic potential (V_s). Also displayed is the energy of the state, N, produced by V_s (in the Koster-Slater approximation) when $V_l = 0$, which is the subject of previous work (Refs. 3–9 in the text). This figure corresponds to a V_l which is composition independent. (b) Schematic illustration of states resulting from the combined potential $V_s + V_l$ (where V_s is treated within the Koster-Slater approximation). In the region where the energies of the N and N_Γ states cross, a splitting into two branches occurs. Here it is assumed that the N_Γ and N_X states are localized in $\vec{k}$ space about their respective minima.

split into two branches. The energy of the lower branch (N_-) is parallel to E_X (the energy of the indirect minima) above this point and to E_Γ below, as observed in experiment. Examination of the momentum amplitudes of these states at $\vec{k}=0$ (which reflects the strength of the radiative transition) manifests a strong mixing of the N_Γ and N amplitudes. Since V_l is assumed to be long range, the $\vec{k}=0$ momentum amplitude of N_Γ is large. This results in a strong enhancement of the transition from the N_- state well above the point in x where $W_N = W_{N_\Gamma}$; even though the *energy* of this state, $E_- \simeq W_N$ in this range, the *amplitude* has strong mixing from N_Γ which overshadows the BSE term [which is proportional to $(E_\Gamma - E_-)^{-1} \simeq (E_\Gamma - W_N)^{-1} \ll 1$ in this range]. Below $W_N \simeq W_{N_\Gamma}$ also, the amplitude of N_- has strong N_Γ character until the point $W_{N_\Gamma} \simeq W_{N_X}$. The upper branch ($N_+$, energy E_+) has a different character. Above $W_N \simeq W_{N_\Gamma}$, $E_+ \simeq W_{N_\Gamma}$ and below $E_+ \simeq W_N$ (which eventually enters the Γ continuum). In the amplitude, the N_Γ and BSE terms enter with different signs. Since $E_+ \to E_\Gamma$ in this case, the magnitude of the BSE term increases until it cancels the contribution from N_Γ for some x below that where $W_N \simeq W_{N_\Gamma}$. At still lower x, the BSE term dominates, so that the $\vec{k}=0$ amplitude of N_+ diverges as $E_+ \to E_\Gamma$. When $W_{N_\Gamma} \simeq W_{N_X}$, a similar phenomenon occurs. These are discussed in detail in Sec. II.

Until now, we have not specified a model of the long-range potential, V_l, because the features we have discussed are general. The origin of such a potential is not clear. If, however, there exists a region of expansion of lattice constant surrounding the nitrogen atom, then, according to the deformation potential ideas of Bardeen and Shockley,[20] an attractive potential, $E_{1n}\Delta(\vec{r})$ is produced [$E_{1n} < 0$ is the deformation potential constant, and $\Delta(\vec{r})$ is the dilatation, $\equiv\delta$ (volume)/volume classically]. If Δ varies slowly over a wide region, we have an origin of the bound states associated with the Γ (strong $\vec{k}=0$ components) and X (weak $\vec{k}=0$ components). In Sec. III, we model $V_l = E_{1n}\Delta(\vec{r})$ by a square-well potential of strength U and radius a. Applying this model to experimental data[18] at $x \simeq 0.35$, where both N_X and N_Γ states are observed, yields $U = -0.262$ eV and $a = 24.79$ Å. The magnitude of this radius indicates that the N_Γ and N_X wave functions are strongly localized in $\vec{k}$ space (with the same degree of localization as for hydrogenic states) about the Γ and X minima, respectively, and that the potential has weak components with high $\vec{k}$ (so that the effective-mass approximation applies). In addition, this value of U indicates that $\Delta \simeq 3\delta(d)/d \lesssim 0.026$ (d is the lattice constant) so that $\delta(d)/d \simeq 0.9\%$. A simple one-dimensional spring model indicates that the ~18% contraction in going from GaP to GaN would produce ≲2% dilation in cells outside the nitrogen cell in a region of length $2a \sim 50$ Å. Such an expansion, therefore, seems consistent with the potential parameters extracted from experiment.[18] We ignore any effect on the central (nitrogen) cell potential since the matrix element in the Koster-Slater approximation[15] covers a multitude of sins.

The numerical calculations reported in Sec. III bear out our description of the general features of the resulting states and agree with experiment. These points are discussed in Sec. IV.

In short, the theory[19] we present here explains the new experiments[16–18] without any apparent, serious contradictions. We identify the new state

observed with the lower branch, N_ (i.e., see Figs. 1 and 3). Its sudden onset at $x = 0.55$ coincides with the strong increase in radiative transition probability at this composition due to strong coupling to $\vec{k} = 0$ components of the N_Γ state. The fact that all these states exist in the same region of space indicates a large transition probability from N_ to N_X. Thus, in the region $x > 0.55$, where the oscillator strength of N_ is not enhanced, pure population effects,[7] due to the large difference in energies between $E_- \simeq W_N$ and W_{N_X}, could explain the observation of the disappearance of N_ in this range of x. Likewise, such transition probabilities are, in most likelihood, higher than tunneling probabilities to N-N states (which exist in other regions of the crystal) so that the absence of N-N lines may be merely a reflection of their being overwhelmed by N_X because of its high electron population (presumably the N-N states exist at energies comparable to W_{N_X}).

This article is not intended to explain the manner in which disorder could produce such a long-range potential (or, perhaps, region of expansion) which, data indicate,[18] is associated with nitrogen. Instead, we concentrate on showing how the existence of such a potential can explain the experimental data.[16-18] Nevertheless, the insertion of N in crystals of increasing d (decreasing x) would tend to enhance the expansion immediately outside the cell containing the nitrogen; this long-range potential may, therefore, be a product not so much of disorder as of composition effects.

Although the theory described here has been applied to Ga(As, P),[19] it seems likely that it can also explain recent observations in (In, Ga) P:N.[21]

II. GENERAL FEATURES OF STATES INDUCED BY DISORDER AND THE ISOELECTRONIC POTENTIAL

Disorder and lattice-mismatch induced strain can have manifold and complicated effects which are poorly understood. For our purposes, we assume that their major effect in Ga(As, P) is to produce a slowly spatially varying deformation in a large region surrounding the isoelectronic impurity and we neglect all other effects. Then, in accord with the idea of Bardeen and Shockley[20] of the deformation-potential, we can express the energy of the lowest-energy conduction band E_c' in this region as

$$E_c'(\vec{k}) = E_c(\vec{k}) + E_{1n}\Delta(\vec{r}) \ , \tag{2.1}$$

where Δ is the dilatation and E_{1n} the conduction-band deformation-potential constant. The quantity E_c represents the conduction-band dispersion relation in the absence of the deformation. Operationally, we define E_c by empirically measured parameters (e.g., effective masses and energies of conduction-band minima). If the dilatation is such as to increase the lattice constant, the second term in Eq. (2.1) corresponds to an attractive potential.[20] Since the lattice constant in GaN is smaller than that in Ga(As, P), it is plausible that $E_{1n}\Delta$ is attractive. In what follows, we assume that this potential is sufficiently strong and long range to induce bound states associated with the Γ and X conduction-band minima and which are localized in momentum about the respective minima.[19] In this section, we describe the effect of these bound states upon bound states induced by the isoelectronic impurity potential (which is delocalized in momentum) and show that the general features of the spectrum are consistent with experiment.[16-18] Furthermore, in Sec. III, we present numerical calculations which indicate that $E_{1n}\Delta$ is of sufficient magnitude to produce these effects.

The Koster-Slater one-band one-site approximation[15] has been shown[2,3] to provide, at least, a qualitatively correct description of the attractive nitrogen potential in GaP. In order to describe the short-range portion of this potential consistently in Ga(As, P), we employ the same approximation.[4-8] The matrix element of V_s, the short-range portion of the N potential, between Wannier states is given by [4-8]

$$\langle \vec{R}_u, n | V_s | \vec{R}_t, m \rangle = V_0 \delta_{u0} \delta_{t0} \delta_{nc} \delta_{mc} \ , \tag{2.2}$$

where the $\vec{R}_u$ and n correspond, respectively, to the site and band indices of the Wannier states. The nitrogen is located at $\vec{R}_0 = 0$ and we consider coupling to the lowest energy conduction band only, denoted by index c. Let us assume that the total electron potential is $V_c + V_I + V_s$, where V_c denotes the periodic crystal potential and V_I a long-range electron potential (e.g., $V_I = E_{1n}\Delta$). Since we consider V_I and V_s which affect conduction-band states only, a bound state, $|j\rangle$, can be written as

$$|j\rangle = \sum_m |\vec{R}_m, c\rangle \langle \vec{R}_m, c | j \rangle \ , \tag{2.3a}$$

where, in the Koster-Slater approximation,[15,22,23]

$$\langle \vec{R}_m, c | j \rangle = V_0 G(\vec{R}_m, \vec{R}_0, E_j) \langle \vec{R}_0, c | j \rangle \ . \tag{2.3b}$$

The quantity E_j is the energy eigenvalue of $|j\rangle$ and G is the retarded conduction-band Green's function (in the Wannier representation) which obeys the following equation,

$$G(\vec{R}_m, \vec{R}_n, E) \equiv \sum_l \frac{f_l(\vec{R}_m) f_l^*(\vec{R}_n)}{E + i\delta - W_l} \ , \tag{2.3c}$$

$$[E_c(\hbar\vec{\nabla}/i) + V_I(\vec{r}) - W_n] f_n(\vec{r}) = 0 \ . \tag{2.3d}$$

The quantity $\delta \to 0^+$ in our treatment, for simplicity.

In Eq. (2.3d), we have assumed that $V_l(\vec{r})$ is sufficiently slowly varying that the effective-mass approximation[24] holds [i.e., $\langle \vec{R}_m, c | V_l | \vec{R}_n, c \rangle \simeq V_l(\vec{R}_m)\delta_{mn}$]; in addition, we have extended Eq. (2.3d) to continuous $\vec{r}$ values, as is usual in the effective mass approximation[24] instead of the discrete lattice points for which it is strictly valid and represent the eigenvalues of f_l as W_l. The star denotes complex conjugation.

The energy eigenvalues of $|j\rangle$ are given by the solutions of

$$\mathrm{Re}[G(\vec{R}_0, \vec{R}_0, E_j)] = 1/V_0 \ . \tag{2.4a}$$

The amplitude for localization at $\vec{R}_m$ is given by Eq. (2.3b), where, from normalization of the wave function to unity,

$$\langle \vec{R}_0, c | j \rangle = 1 \Big/ \left(\frac{-d}{dE_j} \mathrm{Re}[G(\vec{R}_0, \vec{R}_0, E_j)] \right)^{1/2} \ . \tag{2.4b}$$

The probability amplitude that the electron in $|j\rangle$ has momentum $\vec{k}$ is given by

$$\langle \vec{k}, c | j \rangle = V_0 G(\vec{k}, \vec{R}_0, E_j) \langle \vec{R}_0, c | j \rangle \ , \tag{2.4c}$$

$$G(\vec{k}, \vec{R}, E) \equiv \sum_l C_l(\vec{k}) f_l^*(\vec{R}) / (E + i\delta - W_l) \ , \tag{2.4d}$$

$$C_l(\vec{k}) \equiv \frac{1}{\sqrt{N_0}} \left(\sum_{\vec{R}_n} e^{-i\vec{k}\cdot\vec{R}_n} f_l(\vec{R}_n) \right) \ , \tag{2.4e}$$

where N_0 denotes the number of unit cells in the crystal.

If the potential V_l induces bound states associated with the X and Γ conduction-band minima, denoted by N_X and N_Γ, respectively, then Eq. (2.4a) can be written as

$$V_0 \, \mathrm{Re} \left(\frac{|f_{N_\Gamma}(0)|^2}{E - W_{N_\Gamma} + i\delta} + \frac{|f_{N_X}(0)|^2}{E - W_{N_X} + i\delta} + G_0(0,0,E) \right) = 1 \ . \tag{2.5}$$

In Eq. (2.5), we have denoted the bound-state eigenvalues in Eq. (2.3d) by W_{N_Γ} and W_{N_X} (i.e., $V_s = 0$), and represented the sum over continuum states in Eq. (2.3c) by G_0. In Fig. 1(a), we represent these states schematically on an energy versus composition diagram; the energy of the state N_X is much larger than that of N_Γ because the effective mass at X is much larger than that at Γ. Because of the long-range nature of V_l, these states are localized in momentum about their respective minima, and we ignore the weak hybridization when $W_{N_\Gamma} \simeq W_{N_X}$. We depict, too, in Fig. 1(a), the energy W_N of the isoelectronic state $|N\rangle$ arising from Eq. (2.4a) when $V_l = 0$:

$$\mathrm{Re}[\Lambda(W_N)] = 1/V_0 \ , \tag{2.6a}$$

$$\Lambda(E) \equiv \frac{1}{N_0} \sum_{\vec{k}} \frac{1}{E_c(\vec{k}) - E + i\delta} \ . \tag{2.6b}$$

We determine V_0 from the solution of Eqs. (2.6) in GaP. This state becomes resonant as in earlier studies. In accord with experiment, we assume that $W_{N_X} \ll W_N$. Previous studies of the problem have concentrated upon the properties of $|N\rangle$: because of the short range of V_s, $|N\rangle$ is delocalized in momentum.

We can easily understand the qualitative features of the states arising from the solutions of Eq. (2.5). Writing G_0 as an integral over ρ_c, the local density of states without bound states in the conduction band, we have

$$G_0(0,0,E) = \int_{-\infty}^{\infty} dt \, \rho_c(t) / (E - t + i\delta) \ . \tag{2.7}$$

Although the continuous spectrum is influenced by V_l (e.g., resonances and antiresonances), $G_0 \simeq \Lambda$ deep in the gap, where it is independent of the details of the density of states (V_l induces *one* bound state associated with each conduction-band minimum and the total number of continuum states in the conduction band is $N_0 - 2 \simeq N_0$, since the total number of bound and continuum states is N_0). Since we are interested in values of G_0 in the gap [we desire the bound-state solutions of Eq. (2.5)], we assume that $G_0 \simeq \Lambda$ throughout this region in our calculations.

In Fig. 2, we illustrate schematically the salient features of the solutions of Eq. (2.5) for the "weak-coupling" case (i.e., $|f|^2$ is small and the bound-state terms are local in energy). The dotted curve corresponds to the left-hand side of Eq. (2.5) and the solid curve represents $V_0 \, \mathrm{Re} G_0$. We let $G_0 \simeq \Lambda$ so that $V_0 \, \mathrm{Re}[G_0(0,0,W_N)] = 1$: in other words, the eigenvalue of $|N\rangle$ is unchanged except for the influence of the bound-state terms in Eq. (2.5). The extremely sharp structure of these terms indicates that solutions of Eq. (2.5) exist at approximately the energies W_{N_X}, W_N, and W_{N_Γ} when these energies are well separated: this condition is depicted in Fig. 2(a). When, however, one of the bound-state energies $\simeq W_N$, a splitting into two branches occurs. This is illustrated in Fig. 2(b), where $W_{N_X} \ll W_N \simeq W_{N_\Gamma}$. Denoting the upper and lower branches by N_+ (eigenvalue E_+), and N_- (eigenvalue E_-), respectively, we observe from Fig. 2(a) that, if $W_{N_\Gamma} > W_N$, $E_+ \gtrsim W_{N_\Gamma}$ and $E_- \lesssim W_N$. If, on the other hand, $W_N > W_{N_\Gamma}$, $E_+ \gtrsim W_N$ and $E_- \lesssim W_{N_\Gamma}$. If $W_N \simeq W_{N_\Gamma}$, the $|N_\pm\rangle$ have a strong intermixture of the $|N\rangle$ (delocalized in momentum) and $|N_\Gamma\rangle$ (localized in momentum) states. In general, however, $E_+ \gtrsim \max[W_N, W_{N_\Gamma}]$ and $E_- \lesssim \min[W_N, W_{N_\Gamma}]$. These points are illustrated in Fig. 1(b).

These conclusions, which derive from examining Fig. 2, can be made more quantitative for the weak-coupling case. Assuming that $W_{N_X} \ll W_N, W_{N_\Gamma}$ [as depicted in Fig. 1(a)], we can write, from Eq.

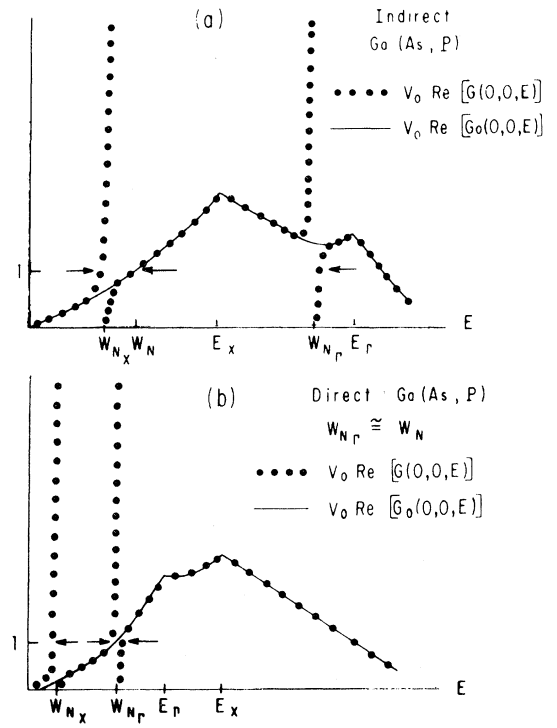

FIG. 2. (a) Schematic illustration in indirect Ga(As, P) of mechanisms governing solution of the eigenvalue Eq. (2.5). The quantities $W_{N\Gamma}$ and W_{N_X} denote the bound-state energies of N_Γ and N_X, respectively, ($V_s = 0$) and W_N denotes the bound-state energy of N($V_l = 0$). These energies are illustrated in Fig. 1(a). When these energies are well separated, the eigenvalues of $V_l + V_s \cong W_i$ (where $i = N_\Gamma$, N_X, and N). The largest (smallest) eigenvalue in this case is always larger (smaller) then any of the W's. The dotted (solid) line represents V_0 times the Green's function with (without) bound states. The arrows indicate eigenvalues. (b) Schematic illustration of mechanisms governing solution of the eigenvalue Eq. (2.5), for $W_{N\Gamma} \simeq W_N$ [see Fig. 1(a)]. The lowest eigenvalue, $E_{N_X} \lesssim W_{N_X}$. At this point, a splitting of N and N_Γ into two branches occurs. The highest, $E_+ \gtrsim \max[W_N, W_{N\Gamma}]$ and the lowest, $E_- \lesssim \min[W_N, W_{N\Gamma}]$. This result depends upon the sharp antisymmetric structure of the bound-state term (dotted line).

(2.5),

$$V_0\left(\frac{|f_{N\Gamma}(0)|^2}{E_\pm - W_{N_\Gamma}} + \mathrm{Re}[\Lambda(E_\pm)]\right) \simeq 1 \ . \tag{2.8}$$

Assuming that $W_N \simeq W_{N_\Gamma}$ (so that $E_+ \simeq W_N$), we can expand Λ about W_N, which yields

$$E_\pm \simeq \frac{1}{2}\left[(W_{N_\Gamma} + W_N) \pm \left((W_{N_\Gamma} - W_N)^2 - 4\,\frac{|f_{N\Gamma}(0)|^2}{\mathrm{Re}[\Lambda'(W_N)]}\right)^{1/2}\right], \tag{2.9a}$$

where $\Lambda' \equiv d\Lambda/dE$. This equation illustrates the splitting into two branches discussed above and supports the conclusions drawn from inspecting Fig. 2. Figure 1(b) depicts the eigenvalues resulting from combining V_s and V_l, and illustrates the splitting, whose magnitude depends upon our model of $|f(0)|^2$, expressed in Eq. (2.9a). Notice that $|N_+\rangle$ becomes resonant higher in energy than $|N\rangle$. For reference, the energies W_{N_X}, $W_{N_\Gamma}(V_s = 0)$ and $W_N(V_l = 0)$ are presented in Fig. 1(a).

Equation (2.9a) represents the energies of the N-like portions of the branches shown in Fig. 1(b) (i.e., by "N-like" we mean $E_\pm \simeq W_N$). For the N_Γ-like portions (i.e., by "N_Γ-like" we mean $E_\pm \simeq W_{N_\Gamma}$), we have, from Eq. (2.8),

$$E_\pm \simeq W_{N_\Gamma} + \frac{V_0|f_{N_\Gamma}(0)|^2}{1 - V_0\,\mathrm{Re}[\Lambda(W_{N_\Gamma})]} \ . \tag{2.9b}$$

A similar expression can be given for E_{N_X}, the solution of Eq. (2.5) corresponding to W_{N_X} (see Fig. 2), for $W_{N_X} \ll W_N, W_{N_\Gamma}$

$$E_{N_X} \simeq W_{N_X} + \frac{V_0|f_{N_X}(0)|^2}{1 - V_0\,\mathrm{Re}[\Lambda(W_{N_X})]} \ . \tag{2.9c}$$

The corresponding expressions for the amplitudes of possessing momentum $\vec{k}$ [Eq. (2.4c)] are given by

$$\langle \vec{k}, c|N_\pm\rangle \simeq \left(\frac{C_{N\Gamma}(k) f_{N_\Gamma}(0)}{E_\pm - W_{N_\Gamma}} + \frac{1/\sqrt{N_0}}{E_\pm - E_c(\vec{k})}\right) \times \{-\mathrm{Re}[\Lambda'(W_N)]\}^{-1/2} , \tag{2.10a}$$

$$\langle \vec{k}, c|N_\pm\rangle \simeq \left(\frac{|V_0 f_{N\Gamma}(0)|/\sqrt{N_0}}{[E_\pm - E_c(\vec{k})]|1 - V_0\,\mathrm{Re}[\Lambda(W_{N_\Gamma})]|} \pm C_{N_\Gamma}(\vec{k})\right) \tag{2.10b}$$

$$\langle \vec{k}, c|N_X\rangle \simeq \left(\frac{|V_0 f_{N_X}(0)|/\sqrt{N_0}}{[E_{N_X} - E_c(\vec{k})]|1 - V_0\,\mathrm{Re}[\Lambda(W_{N_X})]|} - C_{N_X}(\vec{k}) + \frac{|E_{N_X} - W_{N_X}|}{(E_{N_X} - W_{N_\Gamma})}\,\frac{C_{N_\Gamma}(\vec{k}) f_{N_\Gamma}(0)}{|f_{N_X}(0)|}\right) . \tag{2.10c}$$

Equations (2.10a) and (2.10b) correspond, respectively, to the N-like and N_Γ-like branches of N_+ and N_- far away from the region of splitting. The amplitude corresponding to E_{N_X} is given in Eq. (2.10c). In deriving these equations, we have assumed that the energies of the bound states are at least several millivolts from the band edges, so that $\mathrm{Re}\Lambda'$ does not diverge and we have assumed that $f(0)$ and $C(\vec{k})$ are real, as for hydrogenic and square-well states. In addition, we have neglected the effects of V_l on band states and represented them by Bloch states. Since V_l is long range, this is reasonable.

In the neighborhood of the splitting ($W_N = W_{N_\Gamma}$),

the amplitudes are given by

$$\langle \vec{k}, c|N_\pm\rangle \simeq \left(\frac{\{-\mathrm{Re}[\Lambda'(W_N)]\}^{-1/2}}{[E_\pm - E_c(\vec{k})]\sqrt{N_0}} + C_{N_\Gamma}(\vec{k})A_\pm\right)\Big/ B_\pm \ , \tag{2.11a}$$

$$A_\pm \equiv [(E_\pm - W_N)/(E_\pm - W_{N_\Gamma})]^{1/2} \ , \tag{2.11b}$$

$$B_\pm \equiv (1+A_\pm^2)^{1/2} \ . \tag{2.11c}$$

Several interesting points emerge from Eqs. (2.10)–(2.11). First, all the amplitudes involve band-structure enhancement[2] (BSE) terms, as in the usual theory of N in III–V alloys [these are the terms involving $E_c(\vec{k})$]. In addition, these amplitudes mix the appropriate N_Γ and N_X momentum space amplitudes. There is, however, a fundamental difference between the N-like [i.e., Eq. (2.10a)] and the N_Γ-like [i.e., Eq. (2.10b)] branches of $N_\pm$. When the energy $|E_\pm - W_{N_\Gamma}|$ is sufficiently large, the first term in brackets in Eq. (2.10a) is negligible and the amplitude is in precisely the BSE form of earlier treatments of nitrogen. Thus, the properties of the resonant state are unchanged from those deduced from earlier work.[4-7] All the terms in brackets in Eqs. (2.10b) and (2.10c) are *independent* of this energy difference, however. One of the consequences of this BSE dependence is that the N_X amplitude [the N_X state is localized about the X minimum in $\vec{k}$ space, so that $C_{N_X}(0) \simeq 0$] is observable throughout the entire composition range illustrated in Fig. 1. The energy independent BSE term is a direct consequence of the short-range nature of V_s. The energy dependent term in Eq. (2.10a) is consequent upon the fact that the energies of N-like states are sensitive to the Green's function (as in Fig. 2) so that a bound state in their vicinity modifies their character greatly. The energies of N_Γ-like states, however, are largely dependent upon W_{N_Γ}, and are insensitive to another solution of Eq. (2.5) at an energy near W_{N_Γ}.

It is clear that the N-like states do, indeed, achieve the character of short-range ($V_l = 0$) states far from the splitting energy ($W_N \simeq W_{N_\Gamma}$). The term "N_Γ-like" is somewhat misleading, however, since these states possess short-range nature through the admixture of BSE terms. For definiteness, therefore, we refer to N_Γ-like branches and the N_X state as those whose energies are close to the bound-state energies W_{N_Γ} and W_{N_X}, respectively.

An important point to note is that the strong momentum component (C_{N_Γ} is localized in $\vec{k}$ space about the Γ minimum) C_{N_Γ} enhances the N-like $\vec{k}$ amplitude of the N_- state in the region where $W_N \simeq W_{N_\Gamma}$. This occurs because both $E_- - W_{N_\Gamma}$ and $E_- - E_c(\vec{k})$ are negative so that the C_{N_Γ} and BSE terms reinforce each other. In the case of the N_+ amplitude, $E_+ > W_N$ while $E_+ < E_c(\vec{k})$ so that the C_{N_Γ} and BSE terms have opposite signs. As $W_N \to E_\Gamma \equiv E_c(0)$, the BSE term increases in magnitude so that a point is reached where these terms cancel and the zero momentum amplitude, $\langle \vec{k}=0, c|N_+\rangle = 0$. As the band edge is approached more closely, the BSE finally dominates. In the next section, we describe the quantitative consequences of this enhancement.

A final case to consider is that when $W_{N_\Gamma} \simeq W_{N_X}$.[19] As in the previous situation, there is a splitting and, in addition, an admixture of C_{N_Γ} into $\langle \vec{k}, c|N_X\rangle$, which enhances this amplitude. Denoting the upper and lower eigenvalues by D_+ and D_-, respectively, we have,

$$D_\pm \simeq \tfrac{1}{2}[-a_1 \pm (a_1^2 - 4a_2)^{1/2}] \ , \tag{2.12a}$$

$$a_1 \equiv -W_{N_X} - W_{N_\Gamma} - a_3 - a_4 \ , \tag{2.12b}$$

$$a_2 \equiv W_{N_X}W_{N_\Gamma} + a_3 W_{N_X} + a_4 W_{N_\Gamma} \ , \tag{2.12c}$$

$$a_3 \equiv |f_{N_\Gamma}(0)|^2/a_5 \ , \tag{2.12d}$$

$$a_4 \equiv |f_{N_X}(0)|^2/a_5 \ , \tag{2.12e}$$

$$a_5 \equiv 1/V_0 - \Lambda(W_{N_X}) \ . \tag{2.12f}$$

The momentum amplitudes are given by

$$\langle \vec{k}, c|D_\pm\rangle \simeq \left(\frac{C_{N_\Gamma}(\vec{k})f_{N_\Gamma}{}^*(0)}{D_\pm - W_{N_\Gamma}} + \frac{C_{N_X}(\vec{k})f_{N_X}{}^*(0)}{D_\pm - W_{N_X}} + \frac{1/\sqrt{N_0}}{D_\pm - E_c(\vec{k})}\right) \times \left(\frac{|f_{N_\Gamma}(0)|^2}{(D_\pm - W_{N_\Gamma})^2} + \frac{|f_{N_X}(0)|^2}{(D_\pm - W_{N_X})^2}\right)^{-1/2} . \tag{2.13}$$

In this case, $W_{N_\Gamma} \simeq W_{N_X} \ll W_N$ [i.e., see Fig. 1(a)]. Therefore, $V_0\Lambda(D_\pm) < 1$ and we have, from inspecting Fig. 2, $\max[W_{N_\Gamma}, W_{N_X}] \gtrsim D_+$, $D_- \lesssim \min[W_{N_\Gamma}, W_{N_X}]$, and $D_+ > D_-$. For $W_{N_\Gamma} > W_{N_X}$, the upper branch has large $\vec{k}=0$ components [recall that $C_{N_X}(0) \simeq 0$] and the lower has small $\vec{k}=0$ components. If $W_{N_X} > W_{N_\Gamma}$, the situation is reversed. Here, too, there is a region in which $\langle \vec{k}=0, c|D_+\rangle = 0$. At compositions for which $W_{N_X} < W_{N_\Gamma}$, $D_+ < W_{N_\Gamma}$ and $D_- < W_{N_X}$ so that the C_{N_Γ} and BSE terms in Eq. (2.13) are negative for both D_+ and D_-. When, however, $W_{N_\Gamma} \ll W_{N_X}$, $D_- < W_{N_\Gamma} < D_+ < W_{N_X}$. Therefore, the signs of the terms in the D_- amplitude are unchanged and are enhanced by the C_{N_Γ} terms, as in our discussion of the N_- amplitude. The signs of the C_{N_Γ} and BSE terms are opposite, however, in the D_+ amplitude so that there is a region of cancellation (as in the N_+ amplitude) before the BSE dominates.

This discussion applies to the case that the

bound-state term is local in energy (i.e., $|f|^2$ is weak). If $|f|^2$ is strong, however, some of our conclusions about the energies of the N-like branches of $N_\pm$ must be modified. Our discussion of the splittings and the amplitudes is general, however. These points are illustrated in Sec. III, where we perform numerical calculations and to which we proceed.

III. NUMERICAL CALCULATIONS WITHIN THE SQUARE-WELL MODEL OF DISORDER

In Sec. II, we described the general effects of a long-range potential, $V_I = E_{1n}\Delta(\vec{r})$, upon the properties of an isoelectronic state, without specifying details. In this section, we represent V_I by a spherical square-well potential of depth U and radius a centered about the nitrogen-atom lattice site. The results of the previous section depend upon V_I varying so slowly and having such a long range that the effective-mass approximation holds.[24] Obviously, square-well potentials run the gamut from completely local in $\vec{k}$ space (i.e., $a \to \infty$) to completely diffuse in $\vec{k}$ space (i.e., a small). We shall show that numerical results[16-18] consistent with experiment in Ga(As, P):N require that a be large enough (i.e., $a \simeq 25$ Å) that the high $\vec{k}$ Fourier components are small (so that the effective-mass approximation holds) and that the states associated with the Γ and X conduction-band minima are well-localized about these minima in $\vec{k}$ space. Furthermore, values of U consistent with experimental[16-18] Ga(As, P):N energies indicate a dilatation Δ, which is consistent with a maximum average percent increase in lattice constant of $\lesssim 0.9\%$ in the region of greatest disorder.

In order to represent the strength of radiative transition in a concise fashion (without going into details of the calculation of the absorption coefficient, for example), we choose to calculate the $\vec{k}=0$ amplitudes, $\langle \vec{k}=0, c|j\rangle$, given in Eqs. (2.10)–(2.11). The square-well model yields the appropriate quantities for the lowest bound state corresponding to weak coupling,

$$f_{N_i}(0) = k_i \left(\frac{K_i/2\pi}{1+K_i a}\right)^{1/2} , \tag{3.1a}$$

$$C'_{N_i}(0) = 2/\alpha_i K_i f_i(0) a , \tag{3.1b}$$

$$K_i \equiv (2m_i \Delta E_i/\hbar^2)^{1/2} , \tag{3.1c}$$

$$k_i \equiv [2m_i(U-\Delta E_i)/\hbar^2]^{1/2} , \tag{3.1d}$$

$$\alpha_i \equiv 1/[a(K_i^2+k_i^2)^{1/2}] , \tag{3.1e}$$

$$\Delta E_i \equiv E_i - E_{N_i} . \tag{3.1f}$$

The subscript i refers to either Γ or X. The volume of a unit cell is denoted by Ω. In the notation of Sec. II, $C'_{N_X}(\vec{k}) \equiv C_{N_X}(\vec{X}+\vec{k})\sqrt{N_0}$ and $C'_{N_\Gamma} \equiv C_{N_\Gamma}\sqrt{N_0}$.

In order to apply the analysis of Sec. II to Ga(As, P):N, we must specify the Green's function Λ given in Eq. (2.6b). The model we use is different from that employed in previous analyses. In it[25] we describe the conduction band by ellipses of finite extent in momentum, k_Γ and k_X, corresponding, respectively, to the Γ and X minima of E_c. The quantities k_Γ and k_X are determined by requiring that the total number of states in each minimum be equal to that determined by empirical pseudopotential densities of states used in previous work.[4,5] This model yields the following result for Λ,

$$\Lambda(E) = \Lambda_\Gamma(E) + 3\Lambda_X(E) , \tag{3.2a}$$

$$\mathrm{Im}[\Lambda_i(E)] = -(m_i\Omega/2\pi\hbar^2)S_i\Theta(E-E_i) , \tag{3.2b}$$

$$\mathrm{Re}[\Lambda_i(E)] = -(m_i\Omega/\pi\hbar^2)k_i \times \left(1+\frac{r_i}{2}\ln\left|\frac{1-r_i}{1+r_i}\right|\Theta(E-E_i) - |r_i|\tan^{-1}(1/|r_i|)\Theta(E_i-E)\right) , \tag{3.2c}$$

$$r_i \equiv S_i/k_i , \tag{3.2d}$$

$$S_i^2 \equiv 2m_i(E-E_i)/\hbar^2 . \tag{3.2e}$$

In Eqs. (3.2), Θ is the step function [i.e., $\Theta(0)=\frac{1}{2}$, $\Theta(|y|)=1$, $\Theta(-|y|)=0$]. The unit cell volume, $\Omega = [d(x)]^3/4$, where $d(x)$ is the lattice constant in Å, $d(x) = 5.65 - 0.20x$. From fitting to the empirical pseudopotential density of states,[4,5] we find $k_\Gamma = 1.397\,03/d(x)$ and $k_X = 3.797\,33/d(x)$. In numerical calculations, we set $m_\Gamma/m_0 = 0.068 + 0.052x$ and $m_X/m_0 = 0.35$ (m_0 is the free-electron mass). The values for the energies of the band minima are $E_\Gamma = 1.514 + 1.174x + 0.186x^2$ and $E_X = 1.977 + 0.144x + 0.211x^2$ (for $T = 77$ K).

The advantage of this model is that it can be readily extended[25] to treat N-N pairs and incorporate a nonzero width [i.e., $\delta \neq 0^+$ in Eq. (2.6b)]. This is not the case with other Green's function models[3-7] which have been used in the study of the problem of N in III–V alloys. In addition, results for the energy of the isoelectronic N-electron state [i.e., W_N in Eq. (2.6a)] are in at least as good agreement with experiment as those from the other models.[4-7] In particular, this model predicts that the nitrogen state becomes resonant as in earlier work.[4-7]

Composition-dependent energies resulting from an application of these models and Eqs. (2.5)–(2.9) to the Ga(As, P):N experimental data[18] are presented in Fig. 3. The quantity V_0 is determined, as in the past,[4-7] by fixing W_N in GaP; this yields $V_0 = -2.5684$ eV. The square-well parameters are

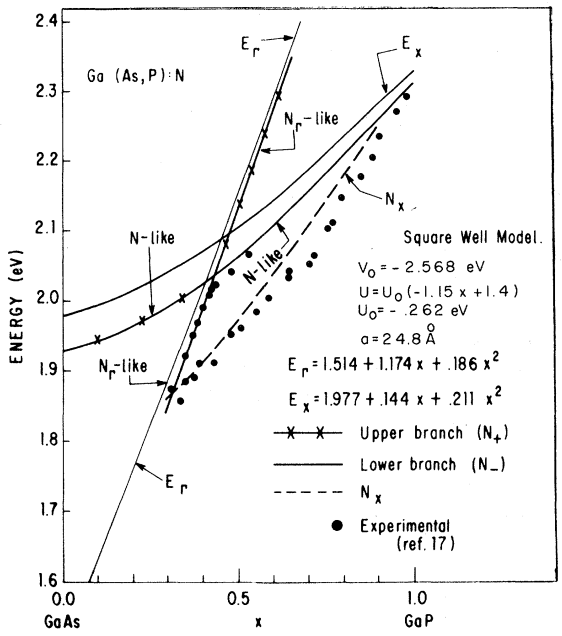

FIG. 3. Composition-dependent energies resulting from application of the theory in Sec. II to a square-well model of strength U and radius a in order to represent the long-range potential V_l. Analysis of experimental energies at $x=0.35$ yields the values of $U \equiv U_0$ and are given in the figure. The x dependence of U presented results from assuming that $U(x=1)=0.25U_0$, which gives a negligible binding energy of the N_X state in GaP. The value of V_0 results from setting $W_N = 0.011$ eV in GaP. The splitting of W_N and W_{N_Γ} is not distinguishable on this figure. In the figure, $V_l = 0$ for $x > 0.9$ and 0.010 eV has been subtracted to represent the bound exciton energy. Agreement with experiment[18] is good, as shown.

determined for states for which both the N_Γ and N_X states are in the gap by observing that the ratio W_{N_Γ}/W_{N_X} depends upon α_Γ and α_X alone [$\alpha_i \propto (Ua^2)^{-1/2}$] for the square-well ground state and not U and a separately. The potential U is determined from $W_{N_i} = U\cos^2(k_i a)$, where $\sin(k_i a) = \alpha_i(k_i a)$ [such that $\cot(k_i a) < 0$]. Applying this procedure to experimental data[18] at $x \simeq 0.35$ yields $U = -0.2623$ eV $\equiv U_0$ and $a = 24.79$ Å. The same method can be applied to the entire composition range in which the N_Γ and N_X states are observed.[16-18] Since this range is small, we choose to fix a at this value and allow U to vary linearly in composition so that $U(x=1)/U_0 = 0.25$ (which gives a state of negligible binding energy in GaP). If we represent $V_l = E_{in}\Delta$,[20] U_0, which is close to the maximum potential, results in a compression $\Delta = \delta(\text{volume})/\text{volume} \simeq +3\delta[d(x)]/d(x) \simeq 0.026$ for $|E_{in}| = 10$ eV. This corresponds to a percent lattice constant dilation of $\simeq 0.9\%$ in the region of the potential. The radius $a \simeq 25$ Å corresponds, approximately, to a cube which has nine unit cells on a side. If we consider the atoms within a simple one-dimensional spring model (all of the same spring constant) in which all the forces are balanced, then a contraction of 18% (which is approximately that in going from GaP to GaN) in the central (N) cell would correspond to ~2% dilation of the lattice constant in each unit cell within the region of the potential outside the central cell. Thus, this effect is consistent with the potential parameters extracted from experiment, at least within this crude analysis. In addition, the $C_{N_i}(\vec{k})$ have the same degree of localization in $\vec{k}$ space as hydrogenic states and the Fourier transform of V_l has weak high $\vec{k}$ components, lending support to our use of the effective-mass approximation.[24]

The theoretical energies displayed in Fig. 3 [which are calculated from Eqs. (2.6) and (2.9)] manifest the splitting into branches which is described in detail in Sec. II (on the scale shown, the splitting is not easily seen). For ease of comparison with experiment, all of the nitrogen state energies in Fig. 3 incorporate a 0.01 eV decrease in order to represent the bound exciton energy.[3] In addition, we set $V_l = 0$ for $0.9 < x$ in order to agree with experimental data,[11,12] which shows N-N structure in this region. The resulting comparison with experiment in Fig. 3 is very good.

The absolute magnitudes of the $\vec{k}=0$ amplitudes as functions of composition which result from this model are presented on a semilog scale in Fig. 4. The amplitudes are calculated from Eqs. (2.10), (2.11), and (2.13) and discussed in Sec. II. Manifest here is the enhancement of the lower (N_-) branch (for $0.4 < x < 0.55$) due to the large $\vec{k}=0$ component [C_{N_Γ} in Eqs. (2.10)–(2.11)] of the N_Γ state as the N-state (energy W_N for $V_l = 0$) approaches the Γ continuum. Displayed, also, is the vanishing of the upper (N_+) amplitude (for $x \sim 0.43$) due to the cancellation of C_{N_Γ} and the band-structure enhancement[2] (BSE) term just before the BSE term begins to diverge (as in previous treatments). Although this vanishing is interesting, it is not likely to be observable because it occurs when $E_+ \simeq E_-$, so that the amplitudes would not be likely to be distinguishable in this region.

The effect of the splitting of the N_X and N_Γ (or N_-) states is apparent for $0.3 \lesssim x \lesssim 0.4$. The lower branch ($N_X$) is enhanced by admixture of C_{N_Γ} and the upper branch displays the onset of the same sort of cancellation apparent for $\langle \vec{k}=0, c | N_+ \rangle$ at $x \cong 0.43$. This cancellation occurs over a wider region than for N_+ because E_{N_X} makes a more acute angle with W_{N_Γ} than does E_+, as is apparent in Fig. 3.

In the experiments,[18] the N_- state does not ap-

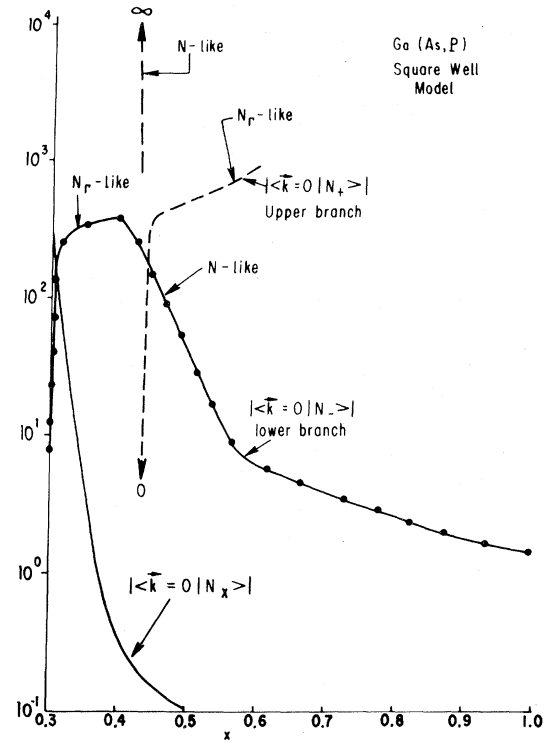

FIG. 4. Representation of absolute magnitude of the $\vec{k}=0$ momentum amplitudes resulting from the parameters of the square-well model. When $x \simeq 0.55$ the amplitude of the lower (N_-) branch increases greatly because of a strong $\vec{k}=0$ component N_Γ in addition to increasing band-structure enhancement (BSE). In the upper branch, N_+, these terms cancel for x slightly greater than the point where W_N enters the Γ continuum (BSE term $\to \infty$). A similar splitting and mixing occurs for $x \gtrsim 0.3$ where $W_{N_X} \to W_{N_\Gamma}$. This figure does not include the point where W_{N_X} reaches E_Γ.

pear until $x \lesssim 0.55$. In addition, the shape of the photoluminescence spectrum is apparently independent of nitrogen concentration,[17] in contrast with what one would expect[1,2] if N-N pairs made an important contribution.

Since all the bound states in our theory correspond to wave functions located in the same region of the crystal, the overlap between them is expected to be much larger than that between single N and N-N pair states. This large overlap results in a large transition probability (short lifetime) between the states (induced, for example, by coupling with phonons). Such a large probability would correspond to a high concentration of electrons in the lower state (because of the large magnitude of $E_- - E_{N_X}$). This reasoning would predict that the radiative recombination from N_X would overwhelm that from N_- until the region where $\langle \vec{k}=0, c|N_-\rangle$ (and, consequently, the oscillator strength) rises precipitously (i.e., $x \lesssim 0.55$ from Fig. 4). In addition, the large number of electrons in N_X would mask the photoluminescence from N-N pairs, which are, presumably, in the same energy range.

Also, the square-well potential can be strong enough to induce higher p states (associated with X). The existence and properties of such states, however, may depend very sensitively on the details of the long-range potential V_l. Because of the undoubted crudeness of our model, we have ignored the possibility of their existence in our analysis (for reference, the p states corresponding to our square-well parameters have binding energies $\simeq 0.050$ eV at $x=0.3$, 0.20 eV at $x=0.5$, and 0.005 eV at $x=0.6$).

In short, this model is in good agreement with experimental observations[16-18] to date. This point is discussed in more detail in Sec. IV.

IV. SYNOPSIS AND CONCLUSIONS

In this article, we have described a theory[19] to explain recent experimental photoluminescence data in Ga(As, P):N.[16-18] These data[17] suggest that, in the region $x < 0.9$, the nitrogen related luminescence is attributable to a single nitrogen isoelectronic state, and associated phonon sidebands, and not pairs. Furthermore, a new higher-energy state appears for $x \lesssim 0.55$.[18] It follows the X minimum until $x \lesssim 0.45$, where it follows the Γ minimum.

We explain these data[16-18] by supposing that a long-range potential strong enough to induce a state N_Γ, energy W_{N_Γ} associated with the Γ minimum and one (N_X, energy W_{N_X}) with the X minimum exists in addition to the usual Koster-Slater short-range nitrogen state (N, energy W_N). In Sec. II, we describe the general features to be expected of the spectrum. Near the region where $W_N = W_{N_\Gamma}$ (composition x_{N_Γ}) the states split into two branches. The lower one, N_- (energy E_-), is of N-like character for $x > x_{N_\Gamma}$ (i.e., $E_- \simeq W_N$) and of N_Γ-like character for $x < x_{N_\Gamma}$ (i.e., $E_- \simeq W_{N_\Gamma}$). Because the strong $\vec{k}=0$ components of N_Γ mix into N_-, this state is enhanced for a composition well above x_{N_Γ}. We, therefore, identify the N_- branch with the new one observed.[18] The N_x state we associate with the lower-energy experimental line.[16-18]

In Sec. III, we report numerical calculations of energies and $\vec{k}=0$ momentum amplitudes for a square-well model (strength U, radius a) of the long-range potential. The results bear out the analysis in Sec. II. Analysis of experimental data at $x \simeq 0.35$ predicts that $U=-0.262$ eV and $a=24.79$ Å. Assuming that the long-range potential (V_l)

arises from an expansion of lattice constant in a volume surrounding the nitrogen and assuming that V_t is a deformation potential[20] yields a percent lattice constant increase $\delta(d)/d \lesssim 0.9\%$ in that region. A crude spring model analysis in a region of length $2a \simeq 50$ Å surrounding the nitrogen predicts $\lesssim 2\%$ expansion outside the nitrogen cell. These results suggest that the potential might result from change in composition, rather than disorder.

Since all the states exist in a single region of the crystal, transition probabilities from N_- to N_X are most likely greater than from N_- to N-N pairs. Thus, since the disappearance of N_- for $x \gtrsim 0.55$[18] coincides with a sizeable decrease in its $\vec{k}=0$ momentum amplitude (the effect of N_Γ decreases), the disappearance may really reflect the competition between electron population effects and oscillator strengths (for $x \gtrsim 0.55$ population effects may dominate, for $x \lesssim 0.55$ oscillator strengths). Likewise, because of the short lifetime for N_--N_X transitions, the resulting large N_X electron population may be much greater than those of the N-N pairs, and the N_X radiation may simply overwhelm that of the pairs (which are presumably at approximately the same energy).

In Fig. 3, the comparison of theoretical square-well model and experimental energies is very good.

It seems, therefore, that the theory presented here can explain all of the experimental data, and, perhaps, lend insight into the effects of disorder in III–V mixed crystal alloys.

ACKNOWLEDGMENT

The author would like to thank Professor N. Holonyak, Jr. for communicating the data in Refs. 16 and 18 prior to publication and for constant encouragement.

*Present address.

[1]M. G. Craford and N. Holonyak, Jr., in *Optical Properties of Solids: New Developments*, edited by B. O. Seraphin (North-Holland, Amsterdam, 1975), Chap. 5.
[2]P. J. Dean, J. Lumin. 1/2, 398 (1970).
[3]R. A. Faulkner, Phys. Rev. 175, 991 (1968).
[4]D. R. Scifres, N. Holonyak, Jr., C. B. Duke, G. G. Kleiman, A. B. Kunz, M. G. Craford, W. O. Groves, and A. H. Herzog, Phys. Rev. Lett. 27, 191 (1971).
[5]D. R. Scifres, H. M. Macksey, N. Holonyak, Jr., R. D. Dupuis, G. W. Zack, C. B. Duke, G. G. Kleiman, and A. B. Kunz, Phys. Rev. B 5, 2206 (1972).
[6]C. B. Duke, D. L. Smith, G. G. Kleinman, H. M. Macksey, N. Holonyak, Jr., R. D. Dupuis, and J. C. Campbell, J. Appl. Phys. 43, 5134 (1972).
[7]George G. Kleiman, J. Appl. Phys. 47, 180 (1976).
[8]M. Altarelli, Phys. Rev. B 11, 5031 (1975).
[9]J. J. Coleman, N. Holonyak, Jr., A. B. Kunz, W. O. Groves, D. L. Keune, and M. G. Craford, Solid State Commun. 16, 319 (1975).
[10]D. G. Thomas and J. J. Hopfield, Phys. Rev. 150, 680 (1966).
[11]M. G. Craford, R. W. Shaw, A. H. Herzog, and W. O. Groves, J. Appl. Phys. 43, 4075 (1972).
[12]N. Holonyak, Jr., R. D. Dupuis, H. M. Macksey, M. G. Craford, and W. O. Groves, J. Appl. Phys. 43, 4148 (1972).
[13]N. Holonyak, Jr., D. R. Scifres, R. D. Burnham, M. G. Craford, W. O. Groves, and A. H. Herzog, Appl. Phys. Lett. 19, 254 (1971).
[14]H. M. Macksey, N. Holonyak, Jr., R. D. Dupuis, J. C. Campbell, and G. W. Zack, J. Appl. Phys. 44, 1333 (1973).
[15]G. F. Koster and J. C. Slater, Phys. Rev. 95, 1167 (1954).
[16]D. J. Wolford, B. G. Streetman, R. J. Nelson, and N. Holonyak, Jr., Solid State Commun. 19, 741 (1976).
[17]D. J. Wolford, B. G. Streetman, W. Y. Hsu, J. D. Dow, R. J. Nelson, and N. Holonyak, Jr., Phys. Rev. Lett. 36, 1400 (1976).
[18]R. J. Nelson, N. Holonyak, Jr., J. J. Coleman, D. Lazarus, D. J. Wolford, W. O. Groves, D. L. Keune, M. G. Craford, and B. G. Streetmen, Phys. Rev. B 14, 685 (1976).
[19]George G. Kleiman, R. J. Nelson, N. Holonyak, Jr., and J. J. Coleman, Phys. Rev. Lett. 37, 375 (1976).
[20]J. Bardeen and W. Shockley, Phys. Rev. 80, 72 (1950).
[21]R. J. Nelson and N. Holonyak, Jr., J. Phys. Chem. Solids 37, 629 (1976).
[22]Joseph Callaway, J. Math. Phys. 5, 783 (1964).
[23]Yu A. Izyumov, Adv. Phys. 14, 569 (1965).
[24]J. M. Ziman, *Principles of the Theory of Solids* (Cambridge U.P., London, 1964).
[25]George G. Kleiman (unpublished).